

CASE REPORT

ADVANCED

EDUCATIONAL CLINICAL CASE SERIES

Fingerprinting MINOCA

Unraveling Clues With Quantitative CMR



Saberio Lo Presti, MD,^a Brendan L. Eck, PhD,^b Reza Reyaldean, MD,^a Christopher Nguyen, PhD,^{a,b,c}
W.H. Wilson Tang, MD,^a Scott D. Flamm, MD, MBA,^{a,b} Nicole Seiberlich, PhD,^d Gastao Lima da Cruz, PhD,^{d,e}
Claudia Prieto, PhD,^{e,f} Deborah H. Kwon, MD^{a,b}

ABSTRACT

In the following case series, we describe the clinical presentation of 2 patients with myocardial infarction with nonobstructive coronary arteries with different underlying pathophysiologic mechanisms. In both scenarios, cardiac magnetic resonance (CMR) imaging provided comprehensive tissue characterization with both conventional parametric mapping techniques and CMR fingerprinting. These cases demonstrate the diagnostic utility for CMR to elucidate the underlying etiology and appropriate therapeutic strategy. (**Level of Difficulty: Advanced.**) (J Am Coll Cardiol Case Rep 2023;7:101722) © 2023 Published by Elsevier on behalf of the American College of Cardiology Foundation. This is an open access article under the CC BY-NC-ND license (<http://creativecommons.org/licenses/by-nc-nd/4.0/>).

Myocardial infarction (MI) with nonobstructive coronary arteries (MINOCA) is defined as the presence of acute MI that fulfills the fourth universal definition of MI criteria (based on cardiac biomarkers and corroborative clinical evidence) in the absence of obstructive coronary artery disease (CAD) on invasive coronary

angiography (<50% stenosis).¹ MINOCA accounts for 6% to 15% of all troponin-positive acute coronary syndromes, disproportionately affecting women,¹⁻⁴ and is associated with significant adverse outcomes.² Cardiac magnetic resonance (CMR) is an important noninvasive imaging modality to determine the pattern of acute myocardial injury (ischemic vs nonischemic).⁵⁻⁷ We report 2 cases of MINOCA highlighting the important diagnostic utility of CMR with quantitative parametric mapping, including the promise of CMR fingerprinting (cMRF) (**Figure 1**).⁶

LEARNING OBJECTIVES

- To describe the current definition of MINOCA and diagnostic approach.
- To recognize the role of CMR as a diagnostic imaging modality for the diagnosis of MINOCA.
- To describe the potential role of CMR fingerprinting to augment diagnostic yield.

PATIENT 1

A 54-year-old man with hypertension presented with acute chest pain. Electrocardiogram demonstrated T-wave abnormalities in the inferolateral leads and elevated high-sensitivity cardiac troponin T

From the ^aDepartment of Cardiovascular Medicine, Heart, Vascular, and Thoracic Institute, Cleveland Clinic, Cleveland, Ohio, USA; ^bImaging Institute, Cleveland Clinic, Cleveland, Ohio, USA; ^cCardiovascular Innovation Research Center, Heart, Vascular, and Thoracic Institute, Cleveland Clinic, Cleveland, Ohio, USA; ^dDepartment of Radiology and Department of Biomedical Engineering, University of Michigan, Ann Arbor, Michigan, USA; ^eSchool of Biomedical Engineering and Imaging Sciences, Kings College London, London, United Kingdom; and the ^fSchool of Engineering, Pontificia Universidad Católica de Chile, Santiago, Chile. The authors attest they are in compliance with human studies committees and animal welfare regulations of the authors' institutions and Food and Drug Administration guidelines, including patient consent where appropriate. For more information, visit the [Author Center](#).

Manuscript received August 14, 2022; revised manuscript received November 15, 2022, accepted November 16, 2022.

**ABBREVIATIONS
AND ACRONYMS****CAD** = coronary artery disease**CMR** = cardiac magnetic resonance**cMRF** = cardiac magnetic resonance fingerprinting**ECV** = extracellular volume**GRASE** = gradient and spin echo sequence**LGE** = late gadolinium enhancement**MI** = myocardial infarction**MINOCA** = myocardial infarction with nonobstructive coronary arteries**OCT** = optical coherence tomography

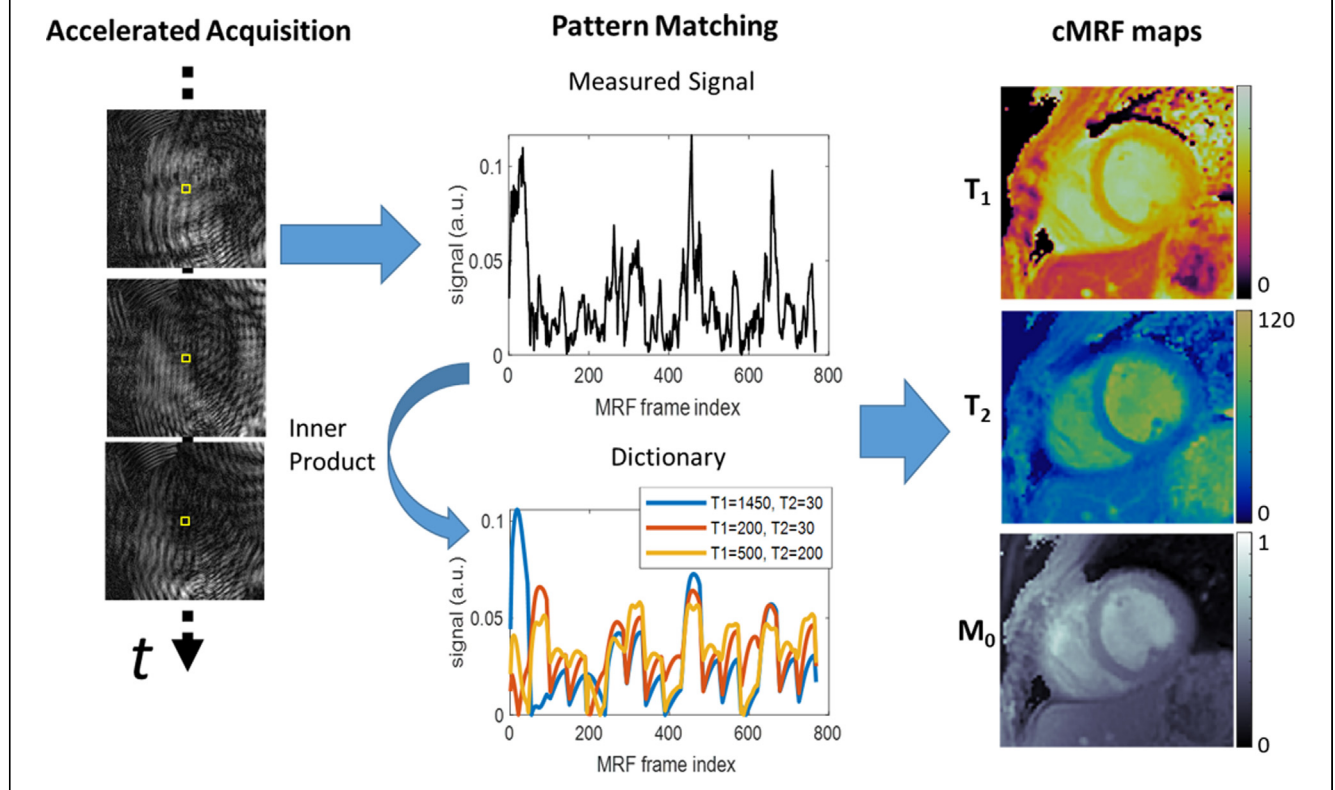
level (0.075 ng/mL; normal range: 0–0.029 ng/mL). Echocardiogram was unremarkable, and coronary angiography revealed nonobstructive CAD (Video 1).

CMR obtained 1 week after symptom onset revealed mid inferolateral and apical lateral wall hypokinesis with near transmural late gadolinium enhancement (LGE) extending into the adjacent pericardium. Because of the paucity of significant risk factors for CAD and the atypical presentation, the diagnosis of myopericarditis was entertained as the likely etiology, and the patient received treatment with colchicine and ibuprofen.

The patient underwent CMR 6 months later, which demonstrated regional wall motion abnormalities and evolution of LGE from a transmural to a subendocardial pattern, which was more consistent with an ischemic insult (Video 2). Modified Look-Locker inversion recovery sequence resulted in prolonged native T_1 time in the midinferolateral segment (1,112

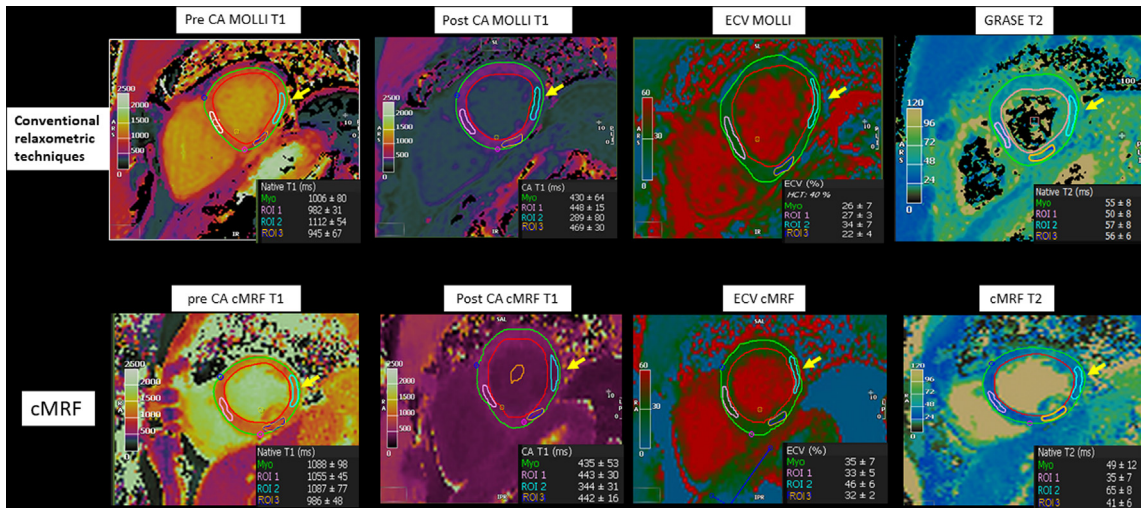
± 54 ms [normal range for 1.5-T: 950 ± 21 ms]).⁸ Postcontrast images demonstrated shortening of T_1 time as well as increased extracellular volume (ECV) (T_1 postcontrast: 289 ± 80 ms; ECV: $34\% \pm 7\%$). T_2 -weighted gradient and spin echo sequence (GRASE) yielded normal T_2 time (Figure 2).⁹ cMRF was also performed, which demonstrated comparable differences to conventional T_1 /ECV mapping while providing simultaneous T_2 measurements within the same slice. Interestingly, cMRF T_2 demonstrated increased T_2 time in the lateral wall, suggestive of persistent myocardial edema (Figure 2). Additional regional tissue deformation analysis demonstrated abnormal peak radial and longitudinal strain of the lateral and immediate adjacent segments (Figure 3).

The constellation of findings was consistent with near transmural ischemic myocardial injury of the inferolateral/lateral wall with concomitant myocardial edema, with interval improvement on follow-up study. Therefore, ibuprofen and colchicine were discontinued, and aspirin was initiated.

FIGURE 1 Accelerated Images Are Reconstructed and Coil-Combined to Produce a Time Series of Image Data

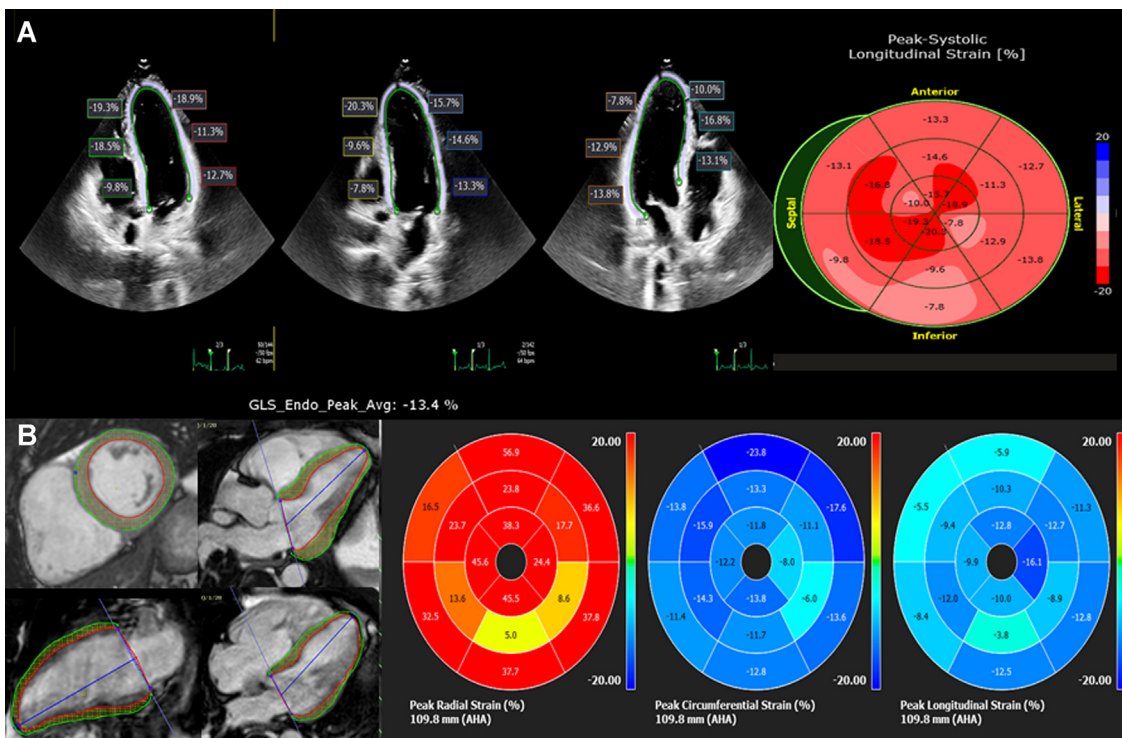
The cardiac magnetic resonance fingerprinting (cMRF) signal for a voxel (yellow box) is measured and compared to a dictionary of signal evolutions for different tissue properties (eg, T_1 , T_2) to find the best match by maximizing the inner product. This procedure is repeated for each voxel to obtain T_1 , T_2 , and M_0 maps. Units: T_1 and T_2 : milliseconds; M_0 : arbitrary units (a.u.).

FIGURE 2 Patient 1 Tissue Analysis

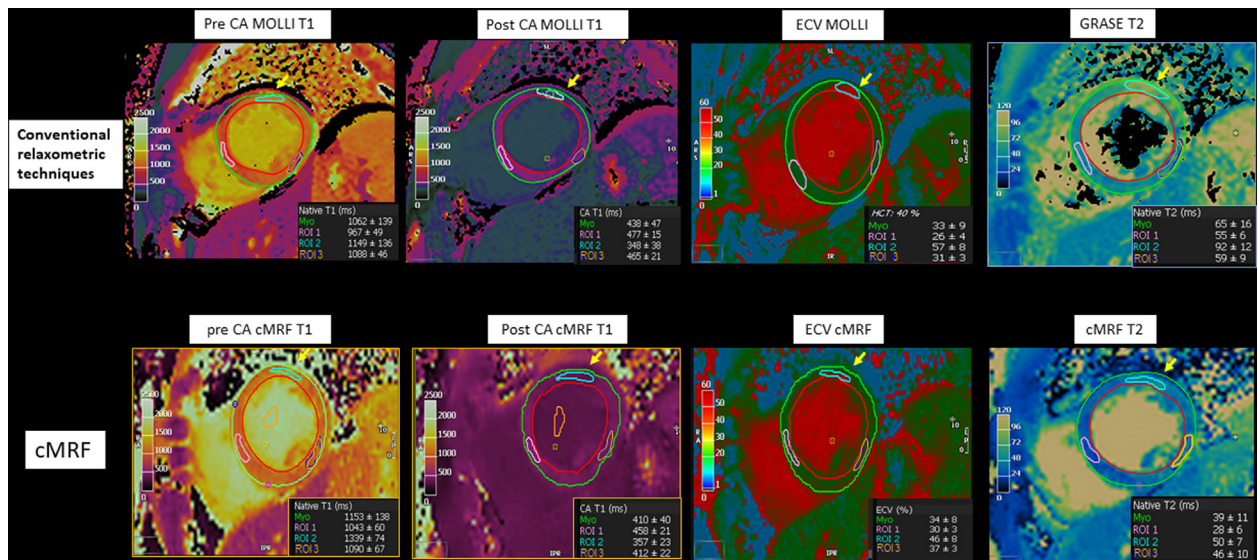


(Upper row) MOLLI pre- and post-CA-generated T₁ and ECV maps demonstrating abnormal values in the midinferolateral segment (region of interest 2, arrow) as well as GRASE sequence T₂-generated maps with normal values. **(Lower row)** cMRF T₁- and ECV-generated maps with similar findings compared with conventional techniques. CA = contrast administration; cMRF = cardiac magnetic resonance fingerprint; ECV = extracellular volume; GRASE = gradient and spin echo sequence; MOLLI = modified Look-Locker inversion recover sequence.

FIGURE 3 Patient 1



(A) Echocardiographic peak longitudinal strain demonstrating low GLS (-13.4%). Note that radial and circumferential strain could not be assessed because of poor echocardiographic windows. **(B)** Peak radial, circumferential, and longitudinal strain polar maps obtained by 3-dimensional cardiac magnetic resonance. AHA = American Heart Association; GLS = global longitudinal strain.

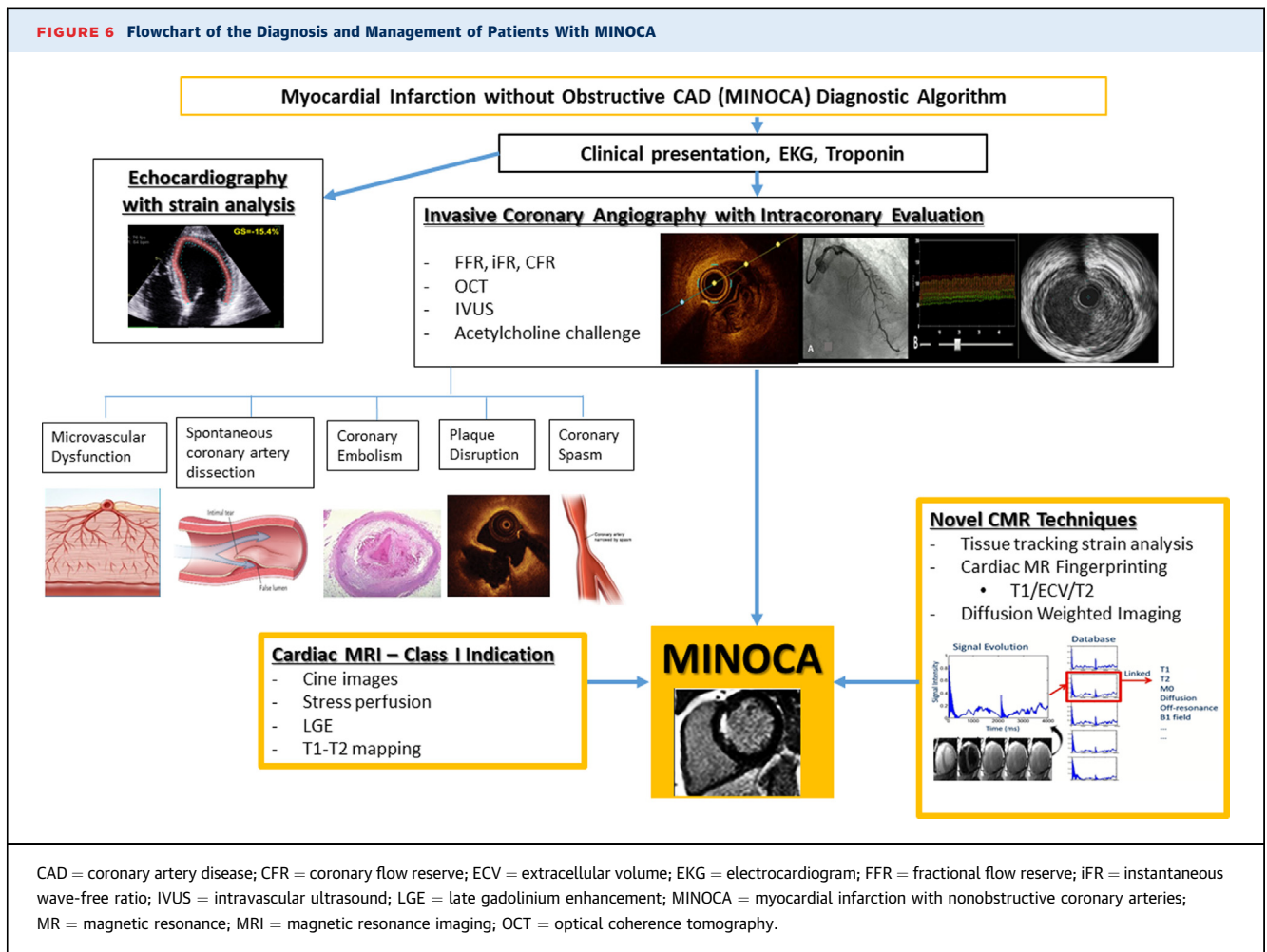
FIGURE 4 Patient 2 Tissue Analysis

(Upper row) MOLLI pre- and post-CA-generated T₁ and ECV maps demonstrating abnormal values in the midanterolateral segment (region of interest 2, arrow) as well as GRASE sequence T₂-generated map consistent with increased edema (region of interest 2). (Lower row) cMRF T₁-, ECV-, and T₂-generated maps with similar findings compared with conventional techniques. Abbreviations as in [Figure 2](#).

EXPERT. Discerning acute ischemic injury vs myocarditis in the setting of normal coronary arteries or nonobstructive CAD can be difficult because both etiologies can potentially present with near transmural LGE with adjacent pericardial inflammation. Parametric mapping may provide additional insights because myocarditis often results in global increases in native T₁/T₂ in addition to focal areas of more significantly increased T₂, whereas MINOCA results in focal native T₁/T₂ elevation in myocardial segments corresponding to the coronary distribution of the infarct-related artery. Because MINOCA often results in smaller areas of myocardial ischemia/infarct, areas of T₂ elevation may also be more focal and may be better discerned with parametric mapping techniques. Differences in breath holds can result in misalignment of conventionally acquired T₁/T₂ data, given that these sequences must be acquired in separate and potentially different breath holds. cMRF provides the ability for simultaneous T₁/T₂ mapping, thus providing precise coregistration to identify focal areas of coexisting increased myocardial fibrosis and edema. Conventional T₁/T₂ mapping and cMRF were not available on the CMR scanner at the hospital where the patient initially presented, thus highlighting the need for standardized CMR protocols to provide optimal quality of care.

PATIENT 2

A 61-year-old woman with hypertension and hyperlipidemia presented with angina. Electrocardiogram demonstrated T-wave abnormalities in the anterolateral leads. Cardiac troponin I level was elevated, and echocardiogram revealed mild left ventricular dysfunction (left ventricular ejection fraction: 48%) with anterolateral wall hypokinesis. Coronary angiography within 10 days of symptom onset demonstrated nonobstructive CAD, without evidence of plaque disruption or dissection on optical coherence tomography (OCT) ([Video 3](#)). There was no evidence of microvascular disease after invasive vasodilator testing with adenosine (coronary flow reserve: 3.6; fractional flow reserve: 0.94). Invasive testing with acetylcholine challenge was remarkable for left anterior descending vasospasm in the absence of symptoms. CMR was obtained 11 days after the initial presentation, which demonstrated mild left ventricular dysfunction (left ventricular end diastolic volume index: 98 mL/m²; left ventricular ejection fraction: 46%), transmural LGE of the midanterolateral and apical lateral walls, and associated hypokinesis ([Video 4](#)). Conventional T₁ mapping demonstrated prolonged native T₁ time and elevated ECV in the midanterolateral wall (1,149 ± 136 ms

FIGURE 6 Flowchart of the Diagnosis and Management of Patients With MINOCA

DISCUSSION

Recent American Heart Association/American College of Cardiology chest pain guidelines have indicated CMR with Class 1 indication for the evaluation of MINOCA, especially when integrated with OCT and cardiac troponin levels, with a diagnostic yield ranging from 85% to 94% while also allowing for risk stratification.^{1,2,10}

Although recent expert consensus excluded nonischemic etiologies in the definition of MINOCA, differentiating this condition from myocarditis and stress-induced cardiomyopathy remains challenging.¹¹ cMRF has emerged as an exciting multiparametric imaging technique that enables simultaneous myocardial T₁ and T₂ mapping in a single breath hold.^{5,6} cMRF thus provides the opportunity to condense tissue characterization imaging protocols

while also providing the opportunity for analysis of the magnetic signal time courses or “fingerprints,” which has shown promising results to better differentiate tissue changes associated with cardiac amyloid deposition compared with conventional T₁/T₂ mapping⁷ and may provide incremental opportunities in the diagnosis of MINOCA. Additional novel CMR techniques, such as diffusion-weighted imaging and perfusion imaging, may provide orthogonal biomarkers to complement myocardial T₁ and T₂ values to better reveal the underlying etiology of acute myocardial injury.¹²

In conclusion, CMR provides important diagnostic utility in patients presenting with suspected MINOCA. Further studies are needed to demonstrate the incremental impact of novel CMR technologies to improve diagnostic yield and/or streamline our current CMR imaging protocols. **Figure 6** outlines a

proposed diagnostic algorithm for patients presenting with presumed MINOCA.

Imaging, and Myocardial Solutions. All other authors have reported that they have no relationships relevant to the contents of this paper to disclose.

FUNDING SUPPORT AND AUTHOR DISCLOSURES

This work was supported through a Philips research agreement with the Cleveland Clinic and a grant from the National Institutes of Health National Institute on Aging (identification K25 AGO70321). Dr Kwon has research agreements with Circle Cardiovascular

ADDRESS FOR CORRESPONDENCE: Dr Deborah Kwon, Heart and Vascular Institute, Cleveland Clinic, 9500 Euclid Avenue, Desk J1, Cleveland, Ohio 44195, USA. E-mail: kwond@ccf.org.

REFERENCES

1. Tamis-Holland JE, Jneid H, Reynolds HR, et al. Contemporary diagnosis and management of patients with myocardial infarction in the absence of obstructive coronary artery disease: a scientific statement from the American Heart Association. *Circulation*. 2019;139:e891-e908.
2. Reynolds HR, Maehara A, Kwong RY, et al. Coronary optical coherence tomography and cardiac magnetic resonance imaging to determine underlying causes of myocardial infarction with nonobstructive coronary arteries in women. *Circulation*. 2021;143:624-640.
3. Gehrie ER, Reynolds HR, Chen AY, et al. Characterization and outcomes of women and men with non-ST-segment elevation myocardial infarction and nonobstructive coronary artery disease: results from the Can Rapid Risk Stratification of Unstable Angina Patients Suppress Adverse Outcomes With Early Implementation of the ACC/AHA Guidelines (CRUSADE) quality improvement initiative. *Am Heart J*. 2009;158:688-694.
4. Berger JS, Elliott L, Gallup D, et al. Sex differences in mortality following acute coronary syndromes. *JAMA*. 2009;302:874-882.
5. Hamilton JI, Jiang Y, Chen Y, et al. MR fingerprinting for rapid quantification of myocardial T1, T2, and proton spin density. *Magn Reson Med*. 2017;77:1446-1458.
6. Eck BL, Flamm SD, Kwon DH, Tang WHW, Vasquez CP, Seiberlich N. Cardiac magnetic resonance fingerprinting: trends in technical development and potential clinical applications. *Prog Nucl Magn Reson Spectrosc*. 2021;122:11-22.
7. Eck BL, Seiberlich N, Flamm SD, et al. Characterization of cardiac amyloidosis using cardiac magnetic resonance fingerprinting. *Int J Cardiol*. 2022;351:107-110.
8. Dabir DCN, Kalra A, Rogers T, et al. Reference values for healthy human myocardium using a T1 mapping methodology: results from the International T1 Multicenter Cardiovascular Magnetic Resonance study. *J Cardiovasc Magn Reson*. 2014;16(1):69.
9. Hanson CA, Kamath A, Gottbrecht M, Ibrahim S, Salerno M. T2 relaxation times at cardiac MRI in healthy adults: a systematic review and meta-analysis. *Radiology*. 2020;297:344-351.
10. Gulati M, Levy PD, Mukherjee D, et al. 2021 AHA/ACC/AASE/CHEST/SAEM/SCCT/SCMR guideline for the evaluation and diagnosis of chest pain: a report of the American College of Cardiology/American Heart Association Joint Committee on Clinical Practice Guidelines. *J Am Coll Cardiol*. 2021;78(22):e187-e285.
11. Pathik B, Raman B, Mohd Amin NH, et al. Troponin-positive chest pain with unobstructed coronary arteries: incremental diagnostic value of cardiovascular magnetic resonance imaging. *Eur Heart J Cardiovasc Imaging*. 2016;17:1146-1152.
12. Paddock S, Tsampasian V, Assadi H, et al. Clinical translation of three-dimensional scar, diffusion tensor imaging, four-dimensional flow, and quantitative perfusion in cardiac MRI: a comprehensive review. *Front Cardiovasc Med*. 2021;8:682027.

KEY WORDS cardiac magnetic fingerprinting, cardiac magnetic resonance, MINOCA

APPENDIX For supplemental videos, please see the online version of this paper.